

The human visual system preserves the hierarchy of 2-dimensional pattern regularity

Peter J. Kohler^{a, b, 1} and Alasdair D. F. Clarke^c

^aYork University, Department of Psychology, Toronto, ON M3J 1P3, Canada; ^bCentre for Vision Research, York University, Toronto, ON, M3J 1P3, Canada; ^cStanford University, Department of Psychology, Stanford, CA 94305, United States; ^dUniversity of Essex, Department of Psychology, Colchester, UK, CO4 3SQ

This manuscript was compiled on September 2, 2020

1 A century of vision research has demonstrated that symmetry contributes to numerous domains of visual perception (1–4). In a 2-D image, the
2 four fundamental symmetries, reflection, rotation, translation and glide reflection, can be combined in 17 distinct ways. These 17 “wallpaper”
3 groups (5–7) obey a hierarchy, determined by mathematical group theory, in which simpler groups are subgroups of more complex ones(8).
4 Here we probe representations of symmetries in wallpaper groups using two methods: (1) Steady-State Visual Evoked Potentials (SSVEPs)
5 recorded using EEG and (2) symmetry detection thresholds measured psychophysically. We find that hierarchical relationships between the
6 wallpaper groups are almost perfectly preserved in both behavior and response amplitudes in visual cortex. This remarkable consistency
7 between the structure of symmetry representations and mathematical group theory, is likely generated over visual development, through
8 implicit learning of regularities in the environment.

Keyword 1 | Keyword 2 | Keyword 3 | ...

1 **S**ymmetries are present at many scales in images of natu-
2 ral scenes, due to a complex interplay of physical forces
3 that govern pattern formation in nature. The importance of
4 symmetry for visual perception has been known at least since
5 the gestalt movement of the early 20th century. Since then,
6 symmetry has been shown to contribute to the perception of
7 shapes (1, 3), scenes (4) and surface properties (2), as well as
8 the social process of mate selection (9). Most of this work has
9 focused on mirror symmetry or *reflection*, with much less attention
10 being paid to the other fundamental symmetries: *rotation*,
11 *translation* and *glide reflection*. In the two spatial dimensions
12 relevant for images, these four fundamental symmetries can be
13 combined in 17 distinct ways, the “wallpaper” groups (5–7).
14 Previous work has focused on four of the wallpaper groups,
15 and used functional MRI to show that rotation symmetries
16 within wallpapers are represented parametrically in several
17 areas in occipital cortex, beginning with visual area V3 (10).
18 This effect is also robust in electroencephalography (EEG),
19 whether measured using Steady-State Visual Evoked Poten-
20 tials (SSVEPs)(10) or event-related paradigms (11). Here we
21 extend on this work by collecting SSVEPs and psychophysical
22 data from human participants viewing the complete set of
23 wallpaper groups. We measure responses in visual cortex to
24 16 out of the 17 wallpaper groups, with the 17th serving as a
25 control stimulus, with the goal of providing a more complete
26 picture of how wallpaper groups are represented in the human
27 visual system.

28 A wallpaper group is a topologically discrete group of isome-
29 tries of the Euclidean plane, i.e. transformations that preserve
30 distance (7). Wallpaper groups differ in the number and
31 kind of these transformations. In mathematical group theory,
32 when the elements of one group is completely contained in
33 another, the inner group is called a subgroup of the outer
34 group (7). Subgroup relationships between wallpaper groups
35 can be distinguished by their indices. The index of a subgroup
36 relationship is the number of cosets, i.e. the number of times
37 the subgroup is found in the outer group (7). As an example,

let us consider groups P6 and P2. If we ignore the translations
in two directions that both groups share, group P6 consists of
the set of rotations $0^\circ, 60^\circ, 120^\circ, 180^\circ, 240^\circ, 300^\circ$, in which
P2 $0^\circ, 180^\circ$ is contained. P2 is thus a subgroup of P6, and
the full P6 set can be generated by every combination of P2
and rotations $0^\circ, 120^\circ, 240^\circ$. Because P2 is repeated three
times in P6, P2 is a subgroup of P6 with index 3 (7). The 17
wallpaper groups thus obey a hierarchy of complexity where
simpler groups are sub-groups of more complex ones (8). The
full set of subgroup relationships is listed in Section 1.4.2 of
the Supplementary Material.

The two datasets presented here puts on in the position
of being able to assess the extent to which both behavior
and brain responses follow that hierarchy. The results show
that activity in human visual cortex is remarkably consist-
ent with the hierarchical relationships between the wallpaper
groups, with SSVEP amplitudes and psychophysical thresh-
olds preserving these relationships at a level that is far beyond
chance. Visual cortex thus appears to encode all of the fun-
damental symmetries using a representational structure that
closely approximates the subgroup relationships from group
theory. Given that most participants had no knowledge of
group theory, the ordered structure of visual responses to
wallpaper groups is likely learned implicitly from regularities
in the visual environment.

Results

The stimuli used in our two experiments were multiple ex-
emplar images belonging to each of the wallpaper groups,
generated from random-noise textures, as described in detail
elsewhere (10). Exemplar images from group P1 was used as
control stimuli, and each exemplar from the other 16 groups
had a power-spectrum matched P1 exemplar. The matched
P1 exemplars were generated by phase-scrambling the exem-
plar images. Because all wallpapers are periodic due to their
lattice tiling structure, the phase-scrambled images all belong

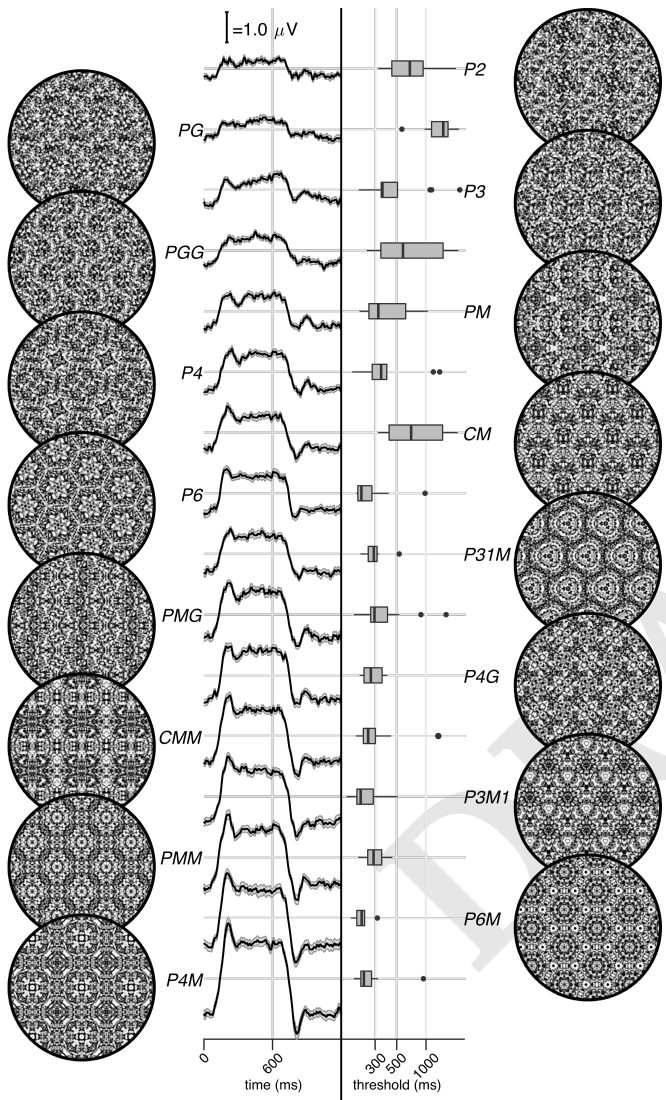
73
74
75
76
77
78
79
80
81
82
83
84
85
86
87

Fig. 1. Examples of each of the 16 wallpaper groups are shown in the left- and right-most column of the figures, next to to the corresponding SSVEP (center-left) and psychological (center-right) data from each group. The SSVEP data are odd-harmonic-filtered cycle-average waveforms. In each cycle, a P1 exemplar was shown for the first 600 ms, followed by the original exemplar for the last 600 ms. Errorbars are standard error of the mean. Psychological data are presented as boxplots reflecting the distribution of display duration thresholds. The 16 groups are ordered by the strength of the SSVEP response, to highlight the range of response amplitudes.

to group P1 regardless of group membership of the original exemplar. P1 contains no symmetries other than translation, while all other groups contain translation in combination with one or more of the other three fundamental symmetries (reflection, rotation, glide reflection) (7). In our SSVEP experiment, this stimulus set allowed us to isolate brain activity specific to the symmetry structure in the exemplar images from activity associated with modulation of low-level features, by alternating exemplar images and control exemplars. In this design, responses to structural features beyond the shared power spectrum, including any symmetries other than translation, are isolated in the odd harmonics of the image update frequency (10, 12, 13). Thus, the combined magnitude of the odd harmonic response components can be used as a measure of the overall strength of the visual cortex response.

The psychophysical experiment took a distinct but related approach. In each trial an exemplar image was shown with its matched control, one image after the other, and the order varied pseudo-randomly such that in half the trials the original exemplar was shown first, and in the other half the control image was shown first. After each trial, participants were told to indicate whether the first or second image contained more structure, and the duration of both images was controlled by a staircase procedure so that a display duration threshold could be computed for each wallpaper group.

A summary of our brain imaging and psychophysical measurements is presented with examples of the wallpaper groups in Figure 1. For our primary SSVEP analysis, we only considered EEG data from a pre-determined region-of-interest (ROI) consisting of six electrodes over occipital cortex (see Supplementary Figure 1.1). SSVEP data from this ROI was filtered so that only the odd harmonics that capture the symmetry response contribute to the waveforms. While waveform amplitude is quite variable among the 16 groups, all groups have a sustained negative-going response that begins at about the same time for all groups, 180 ms after the transition from the P1 control exemplar to the original exemplar. To reduced the amplitude of the symmetry-specific response to a single number that could be used in further analyses and compared to the psychophysical data, we computed the root-mean-square (RMS) over the odd-harmonic-filtered waveforms. The data in Figure 1 are shown in descending order according to RMS. The psychophysical results, shown in box plots in Figure 1, were also quite variable between groups, and there seems to be a general pattern where wallpaper groups near the top of the figure, that have lower SSVEP amplitudes, also have longer psychophysical display duration thresholds.

We now wanted to quantify the degree to which our two measurements were consistent with the subgroup relationships. We hypothesized that more complex groups would (a) produce symmetric-specific SSVEPs with higher amplitudes and (b) shorter display duration thresholds. [PERHAPS WE NEED TO JUSTIFY THESE ASSUMPTIONS] We tested each of these hypotheses using the same approach. We first fitted a Bayesian model with wallpaper group as a factor and participant as a random effect. We fit the model separately for SSVEP RMS and psychophysical data, and then computed posterior distributions for the difference between supergroup and subgroup. These difference distributions could allowed us to compute the conditional probability that the supergroup would produce (a) larger RMS and (b) a shorter threshold

134 durations, when compared to the subgroup. The posterior
 135 distributions are shown in Figure 2 for the SSVEP data, and
 136 in Figure 3 for the psychophysical data, which distributions
 137 color-coded according to conditional probability. For both
 138 data sets our hypothesis is confirmed: For the overwhelming
 139 majority of the 64 subgroup relationships, supergroups are
 140 more likely to produce larger symmetry specific SSVEPs and
 141 shorter threshold durations, and in most cases the conditional
 142 probability of this happening is extremely high.

143 We also ran a control analysis using (1) odd-harmonic
 144 SSVEP data from a six-electrode ROI over parietal cortex (see
 145 Supplementary Figure 1.1) and (2) even-harmonic SSVEP data
 146 from the same occipital ROI that was used in our primary
 147 analysis. By comparing these two control analysis to our
 148 primary SSVEP analysis, we can address the specify of our
 149 effects in terms of location (occipital cortex vs parietal cortex)
 150 and harmonic (odd vs even). For both control analyses (plotted
 151 in Supplementary Figures 3.3 and 3.4), the correspondence
 152 between data and subgroup relationships was weaker than in
 153 the primary analysis. We can quantify the strength of the
 154 association between the data and the subgroup relationships,
 155 by asking what proportion of subgroup relationships that
 156 reach or exceed a range of probability thresholds. This is
 157 plotted in Figure 4, for our psychophysical data, our primary
 158 SSVEP analysis and our two control SSVEP analyses. It is
 159 that odd-harmonic SSVEP data from an occipital ROI and
 160 display duration thresholds both have a strong association
 161 with the subgroup relations, that for a clear majority of the
 162 subgroups survive even at the highest threshold we consider
 163 ($p(\Delta > 0 | \text{data}) > 0.99$), and that the association is far weaker
 164 for the two control analyses.

165 SSVEP data from four of the wallpaper groups (P2, P3,
 166 P4 and P6) was previously published as part of our earlier
 167 demonstration of parametric responses to rotation symmetry
 168 in wallpaper groups(10). We replicate that result using our
 169 Bayesian approach, and find the same parametric effect in
 170 the psychophysical data (Supplementary Figure 4.1 - NEEDS
 171 TO BE LABELED IN THE SM). We also conducted analyses
 172 looking for effects of index and normality in our two datasets,
 173 and found that ... Finally, we conducted a correlation analysis
 174 comparing SSVEP and behavioral data, and found a small
 175 ($R^2 = 0.44$) but above-zero correlation, as indicated by our
 176 confidence intervals. There are several factors that might
 177 explain the relatively weak correlation, most prominently the
 178 fact that the same individuals did not participate in each of
 179 the two experiments. Nevertheless, we find the relationship
 180 between the two datasets interesting, because it suggests that
 181 our psychophysical and SSVEP measurements are tapping
 182 into the same underlying mechanisms.

183 Discussion

184 Here we show that beyond merely responding to the elementary
 185 symmetry operations of reflection (14) and rotation (10),
 186 the visual system explicitly represents hierarchical structure
 187 of the 17 wallpaper groups, and thus the compositions of all
 188 four of the fundamental symmetry transformations (rotation,
 189 reflection, translation, glide reflection) which comprise regular
 190 textures. The RMS measure of SSVEP amplitude, preserves
 191 the complex hierarchy of subgroup relationships among the
 192 wallpaper groups (8). This remarkable consistency was specific
 193 to the odd harmonics of the stimulus frequency, that capture

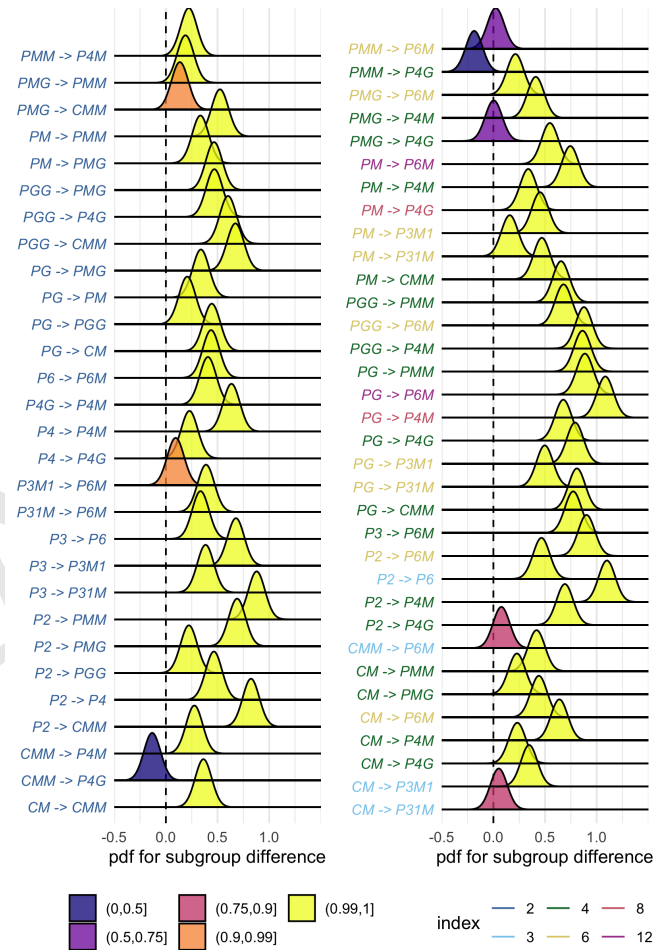


Fig. 2. Posterior distributions for the difference in mean RMS SSVEP response. Colour coding of the text indicates the index of the subgroup, while the colour of the filled distribution relates to the conditional probability that the difference in means is greater than zero. We can see that xx/64 subgroup relationships have $p(\Delta | \text{data}) > 0.9$.

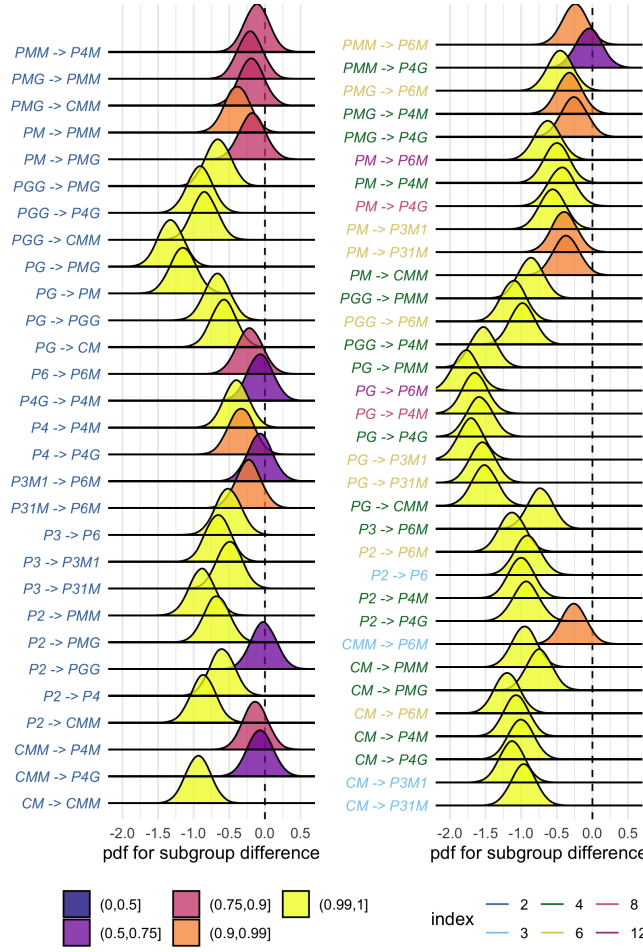


Fig. 3. Posterior distributions for the difference in mean display duration threshold. Colour coding of the text indicates the index of the subgroup, while the colour of the filled distribution relates to the conditional probability that the difference in means is greater than zero. We can see that $xx/64$ subgroup relationships have $p(\Delta|data) > 0.9$.

the symmetry-specific response (10) and to electrodes in an ROI over occipital cortex. When the same analysis was done using the odd harmonics from a parietal cortex ROI (Supplementary Figure 3.4) or using the even harmonics of the occipital cortex ROI (Supplementary Figure 3.4), the data was much less consistent with the subgroup relationships (yellow and green lines, Figure 4).

The current data provide a complete description of the visual system's response to symmetries in the 2-D plane. Our design does not allow us to independently measure the response to P1, but because each of the 16 other groups produce non-zero odd harmonic amplitudes (see Figure 1), we can conclude that the relationships between P1 and all other groups, where P1 is the subgroup, are also preserved by the visual system. The subgroup relationships are not obvious perceptually, and most participants had no knowledge of group theory. Thus, the visual system's ability to preserve the subgroup hierarchy does not depend on explicit knowledge of the relationships. Furthermore, behavioral experiments have shown that although naïve observers can distinguish many of the wallpaper groups (15), they are generally error-prone when asked to assign exemplar images to the appropriate group (16). The correspondence between responses in the visual system and group theory that we demonstrate here, may reflect a form of implicit learning that depends on the structure of the natural world. The environment is itself constrained by physical forces underlying pattern formation and these forces are subject to multiple symmetry constraints (17). The ordered structure of responses to wallpaper groups could be driven by a central tenet of neural coding, that of efficiency. If coding is to be efficient, neural resources should be distributed in such a way that the structure of the environment is captured with minimum redundancy considering the visual geometric optics, the capabilities of the subsequent neural coding stages and the behavioral goals of the organism (18–21). Early work within the efficient coding framework suggested that natural images had a $1/f$ spectrum and that the corresponding redundancy between pixels in natural images could be coded efficiently with a sparse set of oriented filter responses, such as those present in the early visual pathway (22, 23). Our results suggest that the principle of efficient coding extends to a much higher level of structural redundancy – that of symmetries in visual images. The 17 wallpaper groups are completely regular, and relatively rare in the visual environment, especially when considering distortions due to perspective and occlusion. Near-regular textures, however abound in the visual world, and can be approximated as deformed versions of the wallpaper groups (24). The correspondence between brain data and group theory demonstrated here may indicate that the visual system represents visual textures using a similar scheme, with the wallpaper groups serving as anchor points in representational space. This framework resembles norm-based encoding strategies that have been proposed for other stimulus classes, most notably faces (25), and leads to the prediction that adaptation to wallpaper patterns should distort perception of near-regular textures, similar to the aftereffects found for faces (26). Field biologist have demonstrated that animals respond more strongly to exaggerated versions of a learned stimulus, referred to as “supernormal” stimuli (27). In the norm-based encoding framework, wallpaper groups can be considered super-textures, exaggerated examples of the near-

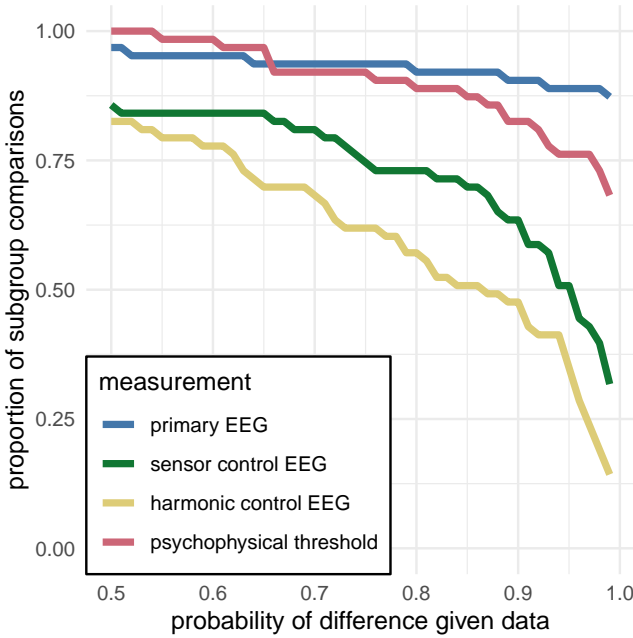


Fig. 4. This plot shows the proportion of subgroup relations that satisfy $p(\Delta > 0 | \text{data}) > x$. We can see that if we take $x = 0.95$ as our threshold, the subgroup relations are preserved in $56/63 = 89\%$ and $49/64 = 78\%$ of the comparisons for the primary EEG and display durations respectively. This compares to the $32/64 = 50\%$ and $22/64 = 35\%$ for the control EEG conditions.

eliminates rotation, reflection and glide-reflection symmetries within each exemplar, but the phase-scrambled images inherit the spectral periodicity arising from the periodic tiling. This means that all control exemplars, regardless of which wallpaper group they are derived from, degenerate to another symmetry group, namely P1. P1 is the simplest of the wallpaper groups, and contains only translations of a region whose shape derives from the lattice. Because the different wallpaper groups have different lattices, P1 controls matched to different groups have different power spectra. Our experimental design takes these differences into account by comparing the neural responses evoked by each wallpaper group to responses evoked by the matched control exemplars.

Stimulus Presentation. Stimulus Presentation. For the EEG experiment, the stimuli were shown on a 24.5" Sony Trimaster EL PVM-2541 organic light emitting diode (OLED) display at a screen resolution of 1920×1080 pixels, 8-bit color depth and a refresh rate of 60 Hz, viewed at a distance of 70 cm. The mean luminance was 69.93 cd/m^2 and contrast was 95%. The diameter of the circular aperture in which the wallpaper pattern appeared was 13.8° of visual angle presented against a mean luminance gray background. Stimulus presentation was controlled using in-house software.

For the psychophysics experiment, the stimuli were shown on a $48 \times 27\text{cm}$ VIEWPixx/3D LCD Display monitor, model VPX-VPX-2005C, resolution 1920×1080 pixels, with a viewing distance of approximately 40cm and linear gamma. Stimulus presentation was controlled using MatLab and Psychtoolbox-3 (30, 31). The diameter of the circular aperture for the stimuli was 21.5° .

EEG Procedure. Visual Evoked Potentials were measured using a steady-state design, in which P1 control images alternated with test images from each of the 16 other wallpaper groups[2]. Exemplar images were always preceded by their matched P1 control image. A single 0.83 Hz stimulus cycle consisted of a control P1 image followed by an exemplar image, each shown for 600 ms. A trial consisted of 10 such cycles (12 sec) over which 10 different exemplar images and matched controls from the same rotation group were presented. For each group type, the individual exemplar images were always shown in the same order within the trials. Participants initiated each trial with a button-press, which allowed them to take breaks between trials. Trials from a single wallpaper group were presented in blocks of four repetitions, which were themselves repeated twice per session, and shown in random order within each session. To control fixation, the participants were instructed to fixate a small white cross in the center of display. To control vigilance, a contrast dimming task was employed. Two times per trial, an image pair was shown at reduced contrast, and the participants were instructed to press a button on a response pad. We adjusted the contrast reduction such that average accuracy for each participant was kept at 85% correct, so that the difficulty of the vigilance task was kept constant.

Psychophysics Procedure. The experiment consisted of 16 blocks, one for each of the wallpaper groups (excluding P1). In each trial, participants were presented with two stimuli (one of which was the wallpaper group for the current block of trials, the other being P1), one after the other (inter stimulus interval of 700ms). After each stimuli had been presented, it

regular textures that surround us. Artists may consciously or unconsciously create supernormal stimuli, to capture the essence of the subject and evoke strong responses in the audience (28). Wallpaper groups are visually compelling and have been widely used in human artistic expression going back to the Neolithic age (29). If wallpapers are super-textures, their prevalence may be a direct consequence of the strategy the human visual system uses for encoding visual textures.

Participants. Twenty-five participants (11 females, mean age 28.7 ± 13.3) took part in the EEG experiment. Their informed consent was obtained before the experiment under a protocol that was approved by the Institutional Review Board of Stanford University. 11 participants (8 females, mean age 20.73 ± 1.21) took part in the psychophysics experiment. All participants had normal or corrected-to-normal vision. Their informed consent was obtained before the experiment under a protocol that was approved by the University of Essex's Ethics Committee.

Stimulus Generation. Exemplars from the different wallpaper groups were generated using a modified version of the methodology developed by Clarke and colleagues(16) that we have described in detail elsewhere(10). Briefly, exemplar patterns for each group were generated from random-noise textures, which were then repeated and transformed to cover the plane, according to the symmetry axes and geometric lattice specific to each group. The use of noise textures as the starting point for stimulus generation allowed the creation of an almost infinite number of distinct exemplars of each wallpaper group. For each exemplar image, phase-randomized control exemplars were generated that had the same power spectrum as the exemplar images for each group. The phase scrambling

345 was masked with white noise for 300ms. After both stimuli had
346 been presented, participants made a response on the keyboard
347 to indicate whether they thought the first or second contained
348 the most symmetry. Each block started with 10 practise trials,
349 (stimulus display duration of 500ms) to allow participants
350 to familiarise themselves with the current block's wallpaper
351 pattern. If they achieved an accuracy of 9/10 in these trials
352 they progressed to the rest of the block, otherwise they carried
353 out another set of 10 practise trials. This process was repeated
354 until the required accuracy of 9/10 was obtained. The rest of
355 the block consisted of four interleaved staircases (using the
356 QUEST algorithm (32), full details given in the SI) of 30 trials
357 each. On average, a block of trials took around 10 minutes to
358 complete.

359 **EEG Acquisition and Preprocessing.** Electroencephalogram
360 Acquisition and Preprocessing. The time-locked Steady-State
361 Visual Evoked Potentials were collected with 128-sensor Hy-
362 droCell Sensor Nets (Electrical Geodesics, Eugene, OR) and
363 were band-pass filtered from 0.3 to 50 Hz. Raw data were eval-
364 uated off line according to a sample-by-sample thresholding
365 procedure to remove noisy sensors that were replaced by the
366 average of the six nearest spatial neighbors. On average, less
367 than 5% of the electrodes were substituted; these electrodes
368 were mainly located near the forehead or the ears. The sub-
369 stitutions can be expected to have a negligible impact on our
370 results, as the majority of our signal can be expected to come
371 from electrodes over occipital, temporal and parietal cortices.
372 After this operation, the waveforms were re-referenced to the
373 common average of all the sensors. The data from each 12s
374 trial were segmented into five 2.4 s long epochs (i.e., each
375 of these epochs was exactly 2 cycles of image modulation).
376 Epochs for which a large percentage of data samples exceeding
377 a noise threshold (depending on the participant and ranging
378 between 25 and 50 μ V) were excluded from the analysis on a
379 sensor-by-sensor basis. This was typically the case for epochs
380 containing artifacts, such as blinks or eye movements. The use
381 of steady-state stimulation drives cortical responses at specific
382 frequencies directly tied to the stimulus frequency. It is thus
383 appropriate to quantify these responses in terms of both phase
384 and amplitude. Therefore, a Fourier analysis was applied on
385 every remaining epoch using a discrete Fourier transform with
386 a rectangular window. The use of epochs two-cycles (i.e., 2.4
387 s) long, was motivated by the need to have a relatively high
388 resolution in the frequency domain, $\delta f = 0.42$ Hz. For each
389 frequency bin, the complex-valued Fourier coefficients were
390 then averaged across all epochs within each trial. Each partic-
391 ipant did two sessions of 8 trials per condition, which resulted
392 in a total of 16 trials per condition.

393 **SSVEP Analysis.** Response waveforms were generated for each
394 group by selective filtering in the frequency domain. For each
395 participant, the average Fourier coefficients from the two ses-
396 sions were averaged over trials and sessions. The Steady-State
397 Visual Evoked Potentials (SSVEP) paradigm we used allowed
398 us to separate symmetry-related responses from non-specific
399 contrast transient responses. Previous work has demonstrated
400 that symmetry-related responses are predominantly found in
401 the odd harmonics of the stimulus frequency, whereas the even
402 harmonics consist mainly of responses unrelated to symme-
403 try, that arise from the contrast change associated with the
404 appearance of the second image[2-4]. This functional distinc-

405 tion of the harmonics allowed us to generate a single-cycle
406 waveform containing the response specific to symmetry, by
407 filtering out the even harmonics in the spectral domain, and
408 then back-transforming the remaining signal, consisting only of
409 odd harmonics, into the time-domain. For our main analysis,
410 we averaged the odd harmonic single-cycle waveforms within
411 a six-electrode region of interest (ROI) over occipital cortex
412 (electrodes 70, 74, 75, 81, 82, 83). These waveforms, averaged
413 over participants, are shown in Figure 2 in the main paper.
414 The same analysis was done for the even harmonics (see Figure
415 S1) and for the odd harmonics within a six electrode ROI over
416 parietal cortex (electrodes 53, 54, 61, 78, 79, 86; see Figure
417 S2). The root-mean square values of these waveforms, for each
418 individual participant, were used to determine whether each
419 of the wallpaper subgroup relationships were preserved in the
420 brain data.

421 **Bayesian Analysis of EEG and Psychophysical data.** Bayesian
422 analysis was carried out using R (v3.6.1) (33) with the **brms**
423 package (v2.9.0) (34) and rStan (v2.19.2 (35)). The data from
424 each experiment were modelled using a Bayesian generalised
425 mixed effect model with wallpaper group being treated as a
426 16 level factor, and random effects for participant. The EEG
427 data and display thresholds were modelled using log-normal
428 distributions with weakly informative, $\mathcal{N}(0, 2)$, priors. After
429 fitting the model to the data, samples were drawn from the pos-
430 terior distribution for each mean of the EEG response (display
431 duration) for each wallpaper group. These samples were then
432 recombined to calculate the distribution of differences for each
433 pair of subgroup and super-group. These distributions were
434 then summarised by computing the conditional probability of
435 obtaining a positive (negative) difference, $p(\Delta|data)$.

436 For further technical details, please see the supplementary
437 materials where the full R code, model specification, prior and
438 posterior predictive checks, and model diagnostics, can be
439 found.

snippets

440 Specifically, the amplitudes of symmetry-specific responses in
441 individual participants ($n = 25$) preserve these relationships
442 at an above-chance level in 88.3% (53 out of 60) of cases.
443

444 we used a steady-state design, in which exemplar images
445 belonging to 16 of the 17 wallpaper groups alternated with
446 phase-scrambled images of the same group. Exemplars from
447 each of the 16 groups alternated at 0.83 Hz with their corre-
448 sponding set of P1 exemplars, that were matched in terms of
449 their Fourier power spectrum.

450 Thus, the magnitude of the odd harmonic response compo-
451 nents can be used as a distance metric for each group, with
452 distance being measured relative to the simplest group, P1.

453 **ACKNOWLEDGMENTS.** Please include your acknowledgments
454 here, set in a single paragraph. Please do not include any acknowl-
455 edgments in the Supporting Information, or anywhere else in the
456 manuscript.

1. Palmer SE (1985) The role of symmetry in shape perception. *Acta Psychologica* 59(1):67–90.
2. Cohen EH, Zaidi Q (2013) Symmetry in context: Salience of mirror symmetry in natural patterns. *Journal of vision* 13(6).
3. Li Y, Sawada T, Shi Y, Steinman R, Pizlo Z (2013) *Symmetry Is the sine qua non of Shape*, Advances in Computer Vision and Pattern Recognition, eds. Dickinson SJ, Pizlo Z. (Springer London), pp. 21–40.
4. Aphantop D, Bell J (2015) Symmetry is less than meets the eye. *Current Biology* 25(7):R267–R268.

- 465 5. Fedorov E (1891) Symmetry in the plane in *Zapiski Imperatorskogo S. Peterburgskogo Mineralogicheskogo Obozchestva* [Proc. S. Peterb. Mineral. Soc.]. Vol. 2, pp. 345–390.
- 466 6. Polya G (1924) XII. Über die analogie der kristallsymmetrie in der ebene. *Zeitschrift für Kristallographie-Crystalline Materials* 60(1):278–282.
- 467 7. Liu Y, Hel-Or H, Kaplan CS, Van Gool L (2010) Computational symmetry in computer vision and computer graphics. *Foundations and Trends® in Computer Graphics and Vision* 5(1–2):1–195.
- 468 8. Coxeter HSM, Moser WOJ (1972) *Generators and relations for discrete groups*, Ergebnisse der Mathematik und ihrer Grenzgebiete ; Bd. 14. (Springer-Verlag, Berlin, New York).
- 469 9. Möller AP (1992) Female swallow preference for symmetrical male sexual ornaments. *Nature* 357(6375):238–240.
- 470 10. Kohler PJ, Clarke A, Yakovleva A, Liu Y, Norcia AM (2016) Representation of maximally regular textures in human visual cortex. *The Journal of Neuroscience* 36(3):714–729.
- 471 11. Kohler PJ, Cottereau BR, Norcia AM (2018) Dynamics of perceptual decisions about symmetry in visual cortex. *NeuroImage* 167(Supplement C):316–330.
- 472 12. Norcia AM, Appelbaum LG, Ales JM, Cottereau BR, Rossion B (2015) The steady-state visual evoked potential in vision research: A review. *Journal of Vision* 15(6):4–4.
- 473 13. Norcia AM, Candy TR, Pettet MW, Vildavski VY, Tyler CW (2002) Temporal dynamics of the human response to symmetry. *Journal of Vision* 2(2):132–139.
- 474 14. Sasaki Y, Vanduffel W, Knutson T, Tyler C, Tootell R (2005) Symmetry activates extrastriate visual cortex in human and nonhuman primates. *Proceedings of the National Academy of Sciences of the United States of America* 102(8):3159–3163.
- 475 15. Landwehr K (2009) Camouflaged symmetry. *Perception* 38:1712–1720.
- 476 16. Clarke ADF, Green PR, Halley F, Chantler MJ (2011) Similar symmetries: The role of wallpaper groups in perceptual texture similarity. *Symmetry* 3(4):246–264.
- 477 17. Hoyle RB (2006) *Pattern formation: an introduction to methods*. (Cambridge University Press).
- 478 18. Attneave F (1954) Some informational aspects of visual perception. *Psychol Rev* 61(3):183–93.
- 479 19. Barlow HB (1961) *Possible principles underlying the transformations of sensory messages*, ed. Rosenblith WA. (MIT Press), pp. 217–234.
- 480 20. Laughlin S (1981) A simple coding procedure enhances a neuron's information capacity. *Z Naturforsch C* 36(9–10):910–2.
- 481 21. Geisler WS, Najemnik J, Ing AD (2009) Optimal stimulus encoders for natural tasks. *Journal of Vision* 9(13):17–17.
- 482 22. Field DJ (1987) Relations between the statistics of natural images and the response properties of cortical cells. *J Opt Soc Am A* 4(12):2379–94.
- 483 23. Olshausen BA, Field DJ (1997) Sparse coding with an overcomplete basis set: a strategy employed by v1? *Vision Res* 37(23):3311–25.
- 484 24. Liu Y, Lin WC, Hays J (year?) Near-regular texture analysis and manipulation in *ACM Transactions on Graphics (TOG)*. (ACM), Vol. 23, pp. 368–376.
- 485 25. Leopold DA, Bonدار IV, Giese MA (2006) Norm-based face encoding by single neurons in the monkey inferotemporal cortex. *Nature* 442(7102):572–5.
- 486 26. Webster MA, MacLin OH (1999) Figural aftereffects in the perception of faces. *Psychon Bull Rev* 6(4):647–53.
- 487 27. Tinbergen N (1953) *The herring gull's world: a study of the social behaviour of birds*. (Frederick A. Praeger, Inc., Oxford, England), pp. xvi, 255.
- 488 28. Ramachandran VS, Hirstein W (1999) The science of art: A neurological theory of aesthetic experience. *Journal of Consciousness Studies* 6(6–7):15–41.
- 489 29. Jablan SV (2014) *Symmetry, Ornament and Modularity*. (World Scientific Publishing Co Pte Ltd, Singapore, SINGAPORE).
- 490 30. Kleiner M, et al. (2007) What's new in psychtoolbox-3. *Perception* 36:1–16.
- 491 31. Brainard DH (1997) Spatial vision. *The psychophysics toolbox* 10:433–436.
- 492 32. Watson AB, Pelli DG (1983) Quest: A bayesian adaptive psychometric method. *Perception & psychophysics* 33(2):113–120.
- 493 33. R Core Team (2019) *R: A Language and Environment for Statistical Computing* (R Foundation for Statistical Computing, Vienna, Austria).
- 494 34. Bürkner PC (2017) Advanced bayesian multilevel modeling with the r package brms. *arXiv preprint arXiv:1705.11123*.
- 495 35. Stan Development Team (2019) RStan: the R interface to Stan. R package version 2.19.2.